JOURNAL OF COMPUTATIONAL PHYSICS 4, 1–18 (1969)

A Numerical Study of Wide-Gap Taylor Vortices

E. H. ROGERS

Rensselaer Polytechnic Institute, Troy, New York 12181

AND

D. W. BEARD

The University of Hull, United Kingdom

Received September 9, 1968

ABSTRACT

Perturbations of solutions of nonlinear equations often are approximated well by eigenfunctions of a linear equation. This suggests the use of truncated eigenexpansions in numerical approximation. This paper describes the successful application of this idea to the numerical approximation of Taylor vortices. These appear as a secondary flow in a viscous, incompressible fluid between concentric, circular rotating cylinders. The expansions used are Fourier expansions of the velocity components with respect to the axial dimension. Comparison with analytic and experimental data, as well as mesh refinements and extension of the number of Fourier components retained, indicate a considerable accuracy with very modest computer storage requirements.

I. INTRODUCTION

Computable approximations for differential equations usually take the form of finite difference equations. Generally, difference approximations are truncated asymptotic expansions in one or more mesh parameters. This suggests the possibility of achieving other computable approximations by truncation of other asymptotic expansions. Indeed series solutions of ordinary differential equations about regular and regular-singular points fit this description; the determination of their coefficients is a purely algebraic matter (they are "computable").

A far less trivial example from hydrodynamic stability is the principal subject of this paper. It is a problem in a broad class fitting the following pattern. Suppose the differential equation $\dot{u}(t) = A_T(t, u(t))$ is descriptive of the behavior of a one parameter ($t \geqslant 0$) family of functions u (in one or more unprinted spatial variables), where A_T is a transformation dependent upon a real quantity T, as well as t and $u(t)$. Suppose further that $A_T(t, 0) = 0$ for all t and T and for some real T_c,

581/4/1-1

$T < T_c$ implies $u(t) = 0$ is asymptotically stable, yet $T > T_c$ implies $u(t) = 0$ is unstable. (Should the stability in question be that of some solution $v(t) \not\equiv 0$, then we may recast the equation as $\dot{w}(t) = B_T(t, w(t)) = -\dot{v}(t) + A_T(t, w(t) + v(t))$ and examine the solution $w(t) = 0$.) When $T > T_c$, solutions initially near the zero solution might be sought as asymptotic expansions $u(t) = 0 + \epsilon u_1(t) + \epsilon^2 u_2(t) + \cdots$ in $\epsilon = 0((T - T_c)^\alpha)$ for some $\alpha > 0$. This leads to a system of equations of the general form

$$\dot{u}_k(t) = A_T^{(k)}(t, u_1(t),..., u_j(t),...), \qquad k = 1, 2,... .$$

The neglect of u_{N+1}, u_{N+2},... requires of us the solution of N equations of this type.

While the resultant system may be more formidable than the original equation, it is not necessarily so. When the asymptotic expansion is simultaneously an eigenfunction expansion, we may be spared the need to deal with certain spatial variables.

II. Taylor Vortices

This paper reports on the flow of a viscous, incompressible fluid between infinite, concentric, circular cylinders rotating at fixed speeds about their common axis. Such flow has been demonstrated both experimentally and theoretically to undergo qualitative changes as, say, the speed of rotation of the inner cylinder is increased from zero with the outer cylinder at rest. The first change is from a laminar (Couette) flow to an axi-symmetric pattern of toroidal vortices (Taylor vortices) stacked one upon another. This transition has been closely studied (see Chandrasekhar [2] and DiPrima [6] for surveys). A second flow transition to a wavy vortex flow at a higher speed has become the subject of study more recently (see Coles [3] and Davey, DiPrima and Stuart [5]).

The steady Couette flow is unmarred by any vortex motion for values of the dimensionless Taylor number T (based on the speed of the inner cylinder, see equation (4)) below a particular critical value T_c. For $T > T_c$ and $T - T_c$ small, asymptotic analyses have shown that the amplitude of the vortex motion is proportional to $(T - T_c)^{1/2}$. In as much as the *steady* Navier-Stokes equations admit Couette flow as a solution for all T, at $T = T_c$ a bifurcation occurs in the solutions of these equations. Thus *nonsteady* flow which tends to a steady state has a choice which is governed by the relative stabilities of Couette flow and vortex flow.

In fact the analytic picture has further relevant detail. Linearization of the equations for a perturbation of Couette flow has led to a boundary-value problem whose solutions are periodic in the axial coordinate z with wave number λ. The time dependence of these solutions is exponential $\exp(\sigma t)$ where $\sigma = \sigma(T, \lambda)$ is a function of Taylor number T and wave number λ. Thus marginally stable solutions (Re $\sigma(T, \lambda) = 0$) occur at various critical T's for various λ. We will denote these

T's by $T_c(\lambda)$ which obeys Re $\sigma(T_c(\lambda), \lambda) = 0$. The T_c referred to previously is the minimum of these and occurs for a unique critical wave number λ_c. This is shown graphically in Fig. 1.

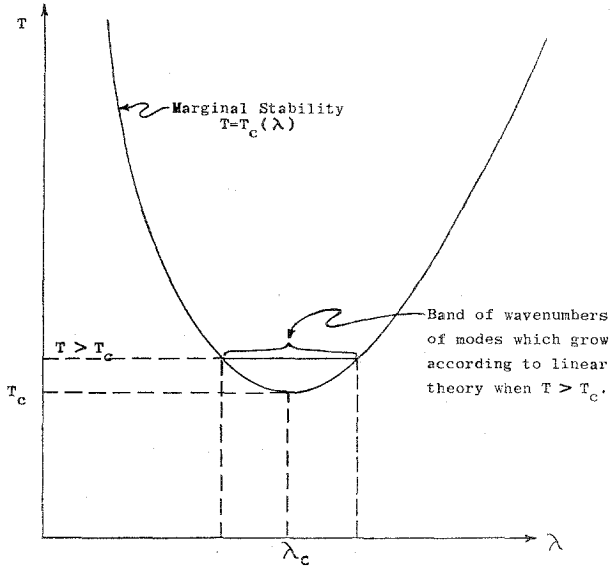

FIG. 1. The curve of marginal stability separating the λ, T plane into regions corresponding to growing and decaying harmonic disturbances of Couette flow according to stability analysis of the linearized equations.

The instability of Couette flow for $T > T_c$ is well-known. Not so well-known are the amplitudes and shapes of the vortex motions which are stable. Extensive analyses (Davey [4], Di Prima [7], Görtler and Velte [10]) have produced asymptotic estimates of both the amplitudes and shapes for $T - T_c$ positive and small. Non-asymptotic information is currently available only through experimental and numerical study. This paper reports a numerical study of Taylor vortices inside a fixed cylinder whose radius is twice that of the rotating inner cylinder. This "wide-gap" situation has been chosen because experiment has shown the stability of the vortex flow for a significant range of T above T_c. The computations reported here are for T in the range $T_c < T < 5T_c$.

Numerical work has been done by Krilov and Proizvolova [11], Capriz, Ghelardoni and Lombardi [1] and Meyer [12] to approximate Taylor vortices. Their studies are based on approximation of the Navier–Stokes equations by differences in the radial, axial and time coordinates (for a fuller discussion see DiPrima and Rogers [8]). The approach used here eliminates axial differencing by

expanding the dependent variables in truncated Fourier series. The resulting system of differential equations for the Fourier amplitudes is differenced for numerical solution.

The use of Fourier expansions is suggested by physical evidence of axial periodicity and by analytical studies of the problem. However, here as in those studies the Fourier expansion imposes a particular axial wavelength $2\pi/\lambda$ upon the calculation. Figure 1 shows that each λ has its own critical Taylor number $T_c(\lambda)$ and when $T > T_c$ there is a band of values λ for which Re $\sigma(T, \lambda) > 0$. Physical flows do not have a particular λ imposed and the mechanism which selects observed wavelengths is not fully understood. The numerical procedure we have selected does permit a direct attack on this wavelength selection problem (see [8]). However, the calculations which we report were carried out with the wavelength $2\pi/\lambda$ fixed as that which Davey [4] reports as the critical wavelength $2\pi/\lambda_c$.

Calculations of torque per unit length on the inner cylinder agree very well with the asymptotic estimates of Davey [4] for T near T_c, while for T farther above T_c our torques exceed Davey's and those obtained experimentally by Donnelly and Simon [9] as well. However, the torques never differ by more than 3 % of the Donnelly and Simon data. Harmonics of the rate of strain at the inner cylinder are calculated and compared with those predicted by Davey's work and experimental data of Snyder and Lambert [13].

In his numerical study Meyer [12] observed the development, with increasing T, of a circumferential shear layer at the vortex faces where the radial flow is outward. He has suggested this as a principal precursor of the transition from axi-symmetric to non-axi-symmetric vortex flow. A related feature would appear to be the growth of a radial jet at the same interfaces noted by Snyder and Lambert [13]. We present corroborating evidence of these developments.

Additional phenomena for which this numerical treatment may prove profitable include thermal convection (the Bénard problem), flame instability, freezing of liquid metals and elastic buckling.

III. Analysis and Discretization of Flow Equations

Let r, θ, z represent cylindrical coordinates, co-axial with the cylinders and let u_r, u_θ, u_z represent the velocity components of the fluid. Cylinders of radii R_1 and R_2 of infinite length bound the fluid ($R_1 < R_2$) and rotate at angular speeds Ω_1, Ω_2, respectively. We let u_r', u_θ', u_z', p' denote perturbations of the velocity and pressure fields from their values in Couette flow. Thus

$$u_r = u_r', \quad u_\theta = V(r) + u_\theta', \quad u_z = u_z' \quad \text{and} \quad p = p' + \int^r \rho \frac{V^2(r)}{r}\, dr \qquad (1)$$

where $V(r) = Ar + Br^{-1}$ and ρ is the density of the viscous, incompressible fluid. The constants A and B are determined by the boundary conditions $u_\theta = R_1\Omega_1$ at $r = R_1$ and $u_\theta = R_2\Omega_2$ at $r = R_2$.

We nondimensionalize our variables via the transformations from r, θ, z to x, θ, ζ and $u_r', u_\theta', u_z', p'$ to u, v, w, p given by

$$\begin{gathered} r = R_0 + xd, \qquad z = \zeta d, \\ u_r' = (-\nu/\alpha d)\, u, \qquad u_\theta' = R_0\Omega_0 v, \qquad u_z' = (-\nu/\alpha d)\, w, \\ p' = (-\nu^2/\alpha d^2)\, p, \end{gathered} \tag{2}$$

where

$$\begin{gathered} R_0 = \tfrac{1}{2}(R_1 + R_2), \qquad d = R_2 - R_1, \qquad \nu \text{ is the kinematic viscosity}, \\ \delta = d/R_0, \qquad \Omega_0 = \tfrac{1}{2}(\Omega_1 + \Omega_2), \qquad \alpha = -2A\delta/\Omega_0. \end{gathered} \tag{3}$$

As additional conveniences we define

$$\begin{gathered} \mu = \Omega_2/\Omega_1, \qquad \eta = R_1/R_2, \qquad \xi(x) = \delta/(1 + \delta x), \\ \Omega_L(x) = \Omega_0^{-1}[A + B/(R_0 + xd)^2], \end{gathered} \tag{4}$$

and the Taylor number $T = -4A\Omega_0 d^4/\nu^2$.

We write the Navier–Stokes equations of incompressible viscous flow and utilize the variables and constants (1), (3) and (4) and transformations (2). Now we impose axi-symmetry (no dependence on θ) and eliminate p from the first and third momentum equations. Finally, we consider only motions which are Fourier-expandable in ζ for all time:

$$\begin{aligned} u &= \sum_{q=1}^{\infty} u_q(r, t) \cos(q\lambda\zeta), \\ v &= v_0(r, t) + \sum_{q=1}^{\infty} v_q(r, t) \cos(q\lambda\zeta), \\ w &= \sum_{q=1}^{\infty} w_q(r, t) \sin(q\lambda\zeta). \end{aligned} \tag{5}$$

In this assumption we are fortunate that in the steady limit the qth Fourier coefficients can be shown to be $O((T - T_c)^{[|q-1|+1]/2})$ as $T \to T_c^+$. The use of cosine series for u reflects our freedom to choose the location of $\zeta = 0$ wherever it suits us in the flow. Having made this choice, we are forced by the continuity equation

to write w in a sine series and by the momentum equations to write v in a cosine series. When amplitudes of like harmonic components are equated, an infinite system of partial differential equations for the $u_q(r, t)$, $v_q(r, t)$, $w_q(r, t)$, and $v_0(r, t)$ results. Use of the expressions for $w_q(r, t)$ obtained from the continuity equation to eliminate the w_q's from all other equations leaves the system

$$\frac{\partial}{\partial t} v_0 - DD^* v_0 = \frac{1}{2\alpha} (D^* + \xi) \sum_{j=1}^{\infty} u_j v_j , \tag{6}$$

$$\frac{\partial}{\partial t} (DD^* - q^2\lambda^2)\, u_q - (DD^* - q^2\lambda^2)^2\, u_q - q^2\lambda^2 T \Omega_L(x)\, v_q = U_q(v_0 , u_1 , v_1 , u_2 , v_2 ,...; \lambda, T, \xi, \alpha, \delta), \tag{7}$$

$$\frac{\partial}{\partial t} v_q - (DD^* - q^2\lambda^2)\, v_q + u_q = V_q(v_0 , u_1 , v_1 , u_2, v_2 ,...; \lambda, T, \xi, \alpha, \delta) \tag{8}$$

for $q = 1, 2,...$. Here $D = \partial/\partial x$, $D^* = D + \xi(x)$ and U_q and V_q represent quadratic terms in the u's and v's (see the appendix). Except for a slight variation in scaling, this is the system of equations derived by DiPrima in [7].

Computation restricts us to a finite subsystem of these equations. The series in the expressions for U_q and V_q are simply terminated by choosing $0 = u_{Q+1} = v_{Q+1} = u_{Q+2} = v_{Q+2} = \cdots$ and restricting q in Eqs. (7) and (8) to $1 \leqslant q \leqslant Q$. This is the promised truncation of asymptotic expansions. The resulting system may be given the form

$$\frac{\partial}{\partial t} (P\mathbf{U}) = M\mathbf{U} + N\mathbf{U} + \mathbf{S}(\mathbf{U}), \tag{9}$$

where $\mathbf{U} = (v_0 , u_1 , v_1 ,..., u_Q , v_Q)^{\mathrm{T}}$, P is a diagonal $(2Q + 1) \times (2Q + 1)$ matrix of operator elements

$$P_{ii} = \begin{cases} 1 & \text{for } i = 0 \text{ and } 2k + 1 \\ DD^* - k^2\lambda^2 & \text{for } i = 2k, \end{cases}$$

$k = 1, 2,..., Q$, M is a diagonal matrix of operator elements

$$M_{ii} = \begin{cases} DD^* - k^2\lambda^2 & \text{for } i = 2k + 1 \text{ (including } k = 0) \\ (DD^* - k^2\lambda^2)^2 & \text{for } i = 2k, \end{cases}$$

$k = 1, 2,..., Q$, and N is a matrix of zeros but for

$$\begin{aligned} N_{i+1\, i} &= -1 && \text{for } i = 2k \\ N_{i\, i+1} &= k^2\lambda^2 T \Omega_L(x) && \text{for } i = 2k, \end{aligned}$$

$k = 1, 2, \ldots, Q$, and

$$\mathbf{S}(\mathbf{U}) = \left(\frac{1}{2\alpha}(D^* + \xi)\sum_{j=1}^{Q} u_j v_j\,,\ U_1\,,\ V_1\,,\ldots,\ U_Q\,,\ V_Q\right)^{\mathrm{T}}.$$

The differencing of these equations is achieved by application of linearity and chain rule until D, D^2, D^3, D^4 apply only to a single unknown dependent variable and then replacement of these derivatives by difference ratios of a "simple-centered" variety (these are defined in the Appendix). For instance, Eq. (6) becomes

$$\begin{aligned}
&\Delta t^{-1}(v_{0j}^{n+1} - v_{0j}^{n}) - \Delta x^{-2}\{\varphi[(1 - \tfrac{1}{2}\Delta x\xi_j)\, v_{0j-1}^{n+1} \\
&\quad - (2 + \Delta x^2\xi_j^2)\, v_{0j}^{n+1} + (1 + \tfrac{1}{2}\Delta x\xi_j)\, v_{0j+1}^{n+1}] \\
&\quad + (1 - \varphi)[(1 - \tfrac{1}{2}\Delta x\xi_j)\, v_{0j-1}^{n} - (2 + \Delta x^2\xi_j^2)\, v_{0j}^{n} + (1 + \tfrac{1}{2}\Delta x\xi_j)\, v_{0j+1}^{n}]\} \\
&= \frac{1}{2\alpha}\sum_{k=1}^{Q}\left[\frac{1}{2\Delta x}(u_{k\,j+1}^{n+1} - u_{k\,j-1}^{n+1})\, v_{kj}^{n+1}\right. \\
&\quad \left. + \frac{1}{2\Delta x}\, u_{kj}^{n+1}(v_{k\,j+1}^{n+1} - v_{k\,j-1}^{n+1}) + 2\xi_j u_{kj}^{n+1} v_{kj}^{n+1}\right]
\end{aligned} \tag{10}$$

for $j = 1, 2, \ldots, J-1$ and $n = 0, 1, 2, \ldots$ and in which $0 \leqslant \varphi \leqslant 1$, $\Delta t > 0$, $\Delta x = 1/J$, $\xi_j = \xi(-\frac{1}{2} + j\Delta x)$ and F_j^n is an intended approximation of $F(-\frac{1}{2} + j\Delta x, n\Delta t)$ for $F = v_0\,, u_k\,, v_k$. Similar procedures lead to difference-equation approximations of Eqs. (7) and (8). These are accompanied by boundary conditions reflecting $u = v = w = 0$ on the cylinders ($x = \pm\frac{1}{2}$) or equivalently $v_0 = u_q = v_q = Du_q = 0$ for $q = 1, 2, \ldots$. These boundary conditions are

$$v_{0j}^{n} = u_{qj}^{n} = v_{qj}^{n} = u_{qj-1}^{n} - u_{qj+1}^{n} = 0$$

for $j = 0$ and J and $n = 0, 1, 2, \ldots$.

In analogy with Eq. (9), these difference equations including boundary conditions may be put in the form

$$\Delta t^{-1}[(\hat{P}\mathbf{U})_j^{n+1} - (\hat{P}\mathbf{U})_j^{n}] = \varphi(\hat{M}\mathbf{U})_j^{n+1} + (1 - \varphi)(\hat{M}\mathbf{U})_j^{n} + N\mathbf{U}_j^{n} + \hat{\mathbf{S}}_j^{n}(\mathbf{U}) \tag{11}$$

for $j = 1, \ldots, J-1$ where $\hat{P}$, $\hat{M}$ are consistent difference approximations of the operators P, M and $\hat{\mathbf{S}}_j^{n}(\mathbf{U})$ is a difference formulation of $\mathbf{S}(\mathbf{U})$.

The parameter φ allows variation of the extent of implicitness built into these difference equations. A stability analysis of the linearized equation ($\hat{\mathbf{S}} = 0$) shows numerical stability for all $\Delta t > 0$ when $\frac{1}{2} \leqslant \varphi \leqslant 1$.

The reader may observe that Eqs. (6)–(8) are invariant under the change of dependent variables $(-1)^q u_q$ for u_q and $(-1)^q v_q$ for v_q. This property carries over

to the difference equations and accounts for shifts of π/λ in the ζ direction which were observed in the computer output of the velocity fields (outward flow $u > 0$ appeared at both $\zeta = 0$ and $\zeta = \pi/\lambda$ in various computations). The shift is apparently determined by the flow pattern with which a computation is started. All output has been normalized so that the radial velocity u is positive at $\zeta = 0$, $x = 0$.

IV. Numerical Technique; Selection of Parameters

Each component of $\mathbf{U}$ is a function of x and t. In the difference formulation each component is represented by $J + 1$ numbers at each time level. Boundary conditions determine two of these so that (11) represents $(J - 1)(2Q + 1)$ equations in an equal number of scalars approximating $\mathbf{U}^{n+1}$. These equations are implicit for all φ because of the differencing demanded by $\hat{P}$. However, we are saved from an imposing task of solution by the diagonal character of the operators P and M. As a result, the difference equation systems for v_0, u_q, v_q may be solved one at a time.

The difference schemes for the operator DD^* in M causes the system of equations for the $v_{0j}^{n+1}(\approx v_0(-\frac{1}{2} + j/J, (n + 1)\,\Delta t))$ and the systems for the $v_{qj}^{n+1}(\approx v_q(-\frac{1}{2} + j/J, (n + 1)\,\Delta t))$ to be tridiagonal while the systems for the u_{qj}^{n+1} are pentadiagonal because of the $(DD^* - q^2\lambda^2)^2$ in M. This simplicity and the time independence of P and M makes the factorization of the coefficient matrices of the $(v_{01}^{n+1},\ldots, v_{0J-1}^{n+1})^{\mathrm{T}}$, $(u_{q1}^{n+1},\ldots, u_{qJ-1}^{n+1})^{\mathrm{T}}$ and $(v_{q1}^{n+1},\ldots, v_{qJ-1}^{n+1})^{\mathrm{T}}$ into triangular factors attractive. It can be accomplished quickly and has to be done just once. Solution of $2Q + 1$ triangular $(J - 1) \times (J - 1)$ systems of equations is performed at each time step for each dependent variable.

Since the convergence to steady state is expected to be an imitation of that which occurs physically, the speed of such convergence is expected to be greater with greater Δt. However, experience with this scheme has shown a conditional stability. A T-dependent upper bound on $\Delta t/(\Delta x)^2$ seems to be required. The convergence did not appear to be greatly affected by its choice, φ was taken to be $\frac{1}{2}$.

The computational effort required to produce a steady flow pattern depends most heavily on the flow pattern which initiates a calculation (that is, the specified initial conditions). Once one steady state was computed, others (corresponding to different T or Q or J) were obtained by calculating a succession of steady states corresponding to intermediate values of the parameters.

Accuracy of the resulting approximations of the steady flow variables is dependent upon Q, the number of Fourier components retained, and upon $J + 1$, the number of mesh points in $-0.5 \leqslant x \leqslant 0.5$. Figures 2 and 3 show the dependence of certain global parameters

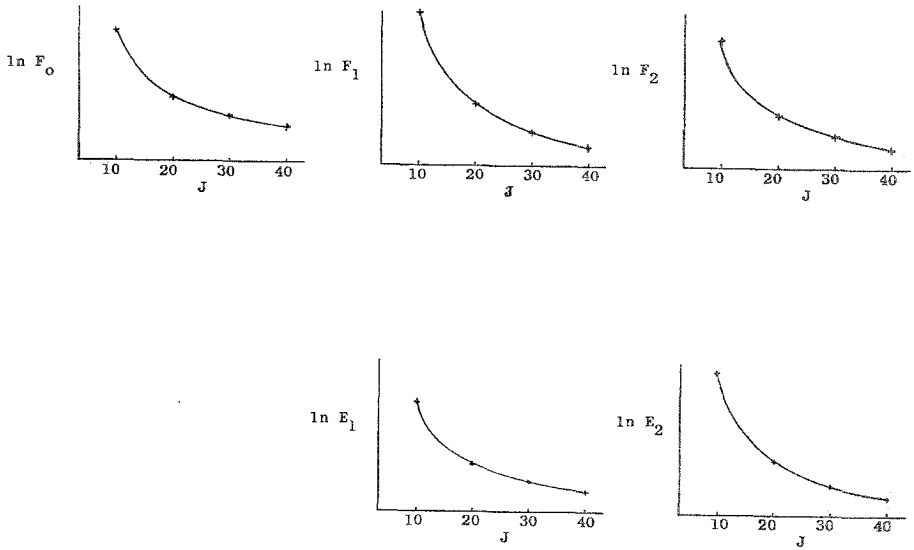

FIG. 2. Logarithms of root-mean-square radial averages of the mean velocity perturbation and various velocity harmonics for various radial mesh intervals (J^{-1}) showing convergence as J grows; for calculations with $T/T_c = 1.29$, $Q = 2$, $R_2 = 2R_1$ and $\Omega_2 = 0$.

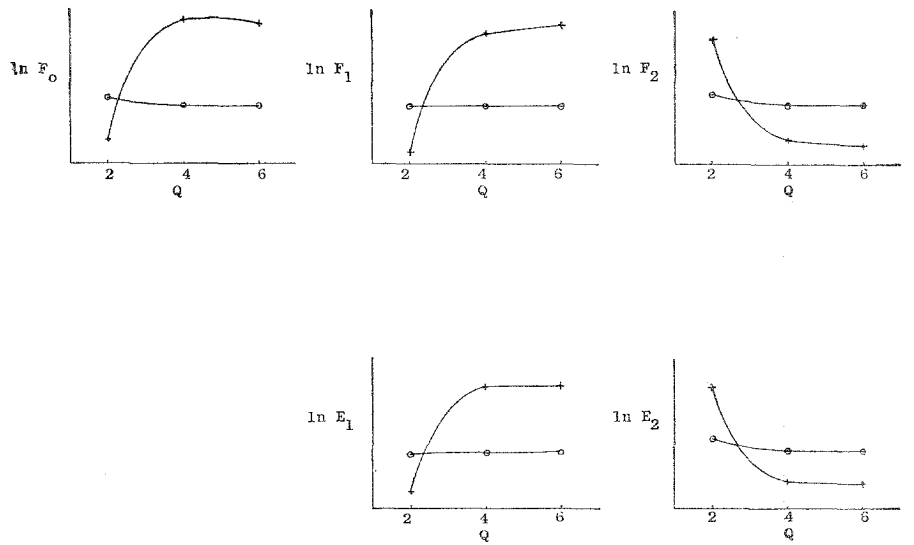

FIG. 3. Logarithms of root-mean-square radial averages of the mean velocity perturbation and various velocity harmonics for various truncations of the Fourier expansions; ⊙ for $T/T_c = 1.29$, + for $T/T_c = 3.226$; $J = 40$, $R_2 = 2R_1$ and $\Omega_2 = 0$.

$$\left(\text{namely,} \quad E_q = \left\{\int_{-0.5}^{0.5} u_q^2 \, dx\right\}^{1/2} \quad \text{and} \quad F_q = \left\{\int_{-0.5}^{0.5} v_q^2 \, dx\right\}^{1/2}\right)$$

of the flow upon Q and J (these calculations were performed with $R_2 = 2\ R_1$ and $\Omega_2 = 0$). These indicate how few Fourier components are required to produce apparent convergence. The comparison between the maximum Q used (namely, 6) and the maximum J (namely, 40) hints at the efficiency of the use of truncated expansions. All results reported in the next section have been obtained with $J = 40$ and with $Q = 6$ for $T \geqslant 1.29\ T_c$ and with $Q = 2$ for $T < 1.29\ T_c$.

V. Computed Taylor Vortices

The validation of the numerical technique in this application is possible only by checking internal consistencies (such as the decay of ln E_i and ln F_i shown in Fig. 2) and by comparing computed and experimental data.

The calculations to be discussed in this section were performed with $R_2 = 2R_1$ and $\Omega_2 = 0$. By extrapolation to zero of the measures E_q and F_q of the harmonic content of the vortex flow, estimates of T_c may be made. However, since an extrapolation can be arranged to predict any number one might wish to report for T_c, we present only a graphic form of our data (Fig. 4), observing that all reasonable estimates will fall very close to 3099.6, the value predicted by linear stability

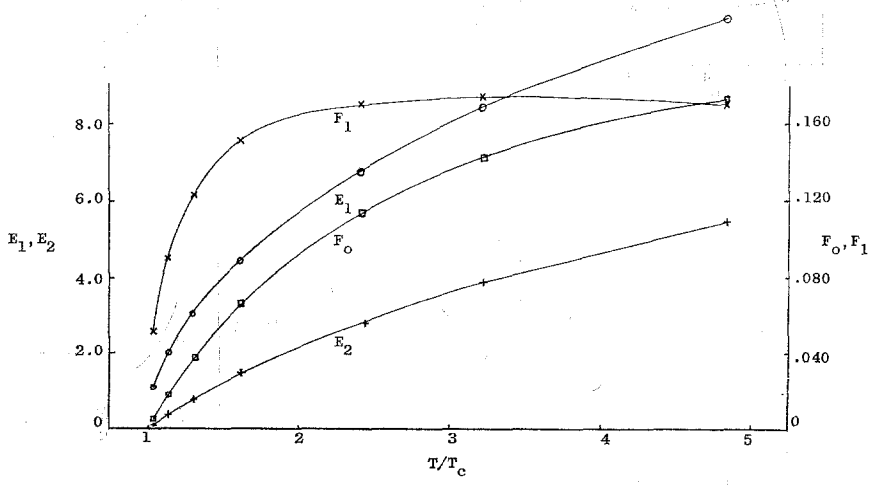

FIG. 4. Root-mean-square radial averages of the mean velocity perturbation and various velocity harmonics versus T/T_c showing decay as $T/T_c \to 1$.

analysis (Davey [4]). An estimate is also possible from our torque data (Fig. 5). Whereever our work has demanded a value for T_c, 3100. has been used.

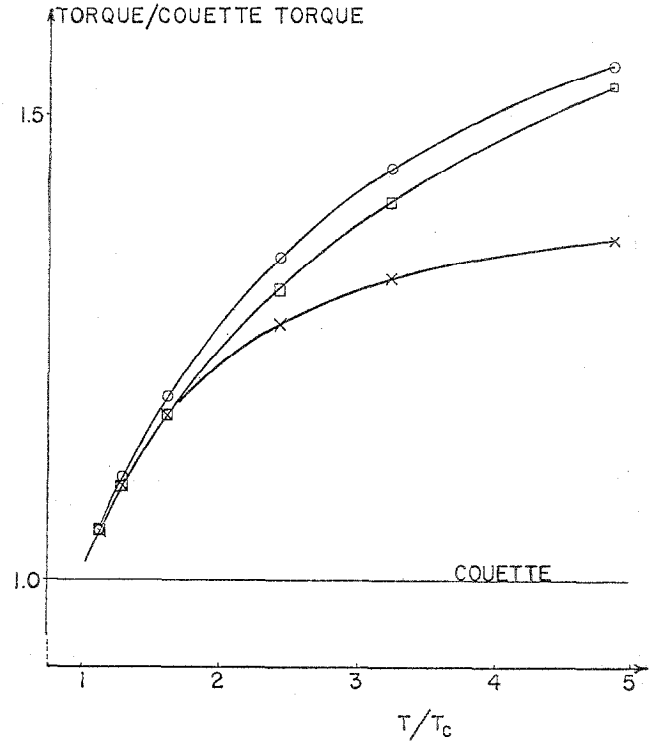

FIG. 5. Non-dimensional torques per unit length versus T/T_c; ⊙—present work; ⊡—Donnelly and Simon; ×—Davey.

An important comparison of theory and experiment is based on calculations of the torque per unit length on the inner cylinder. The torque G is given by

$$G = R_1 \mu h \frac{\lambda}{2\pi} \int_0^{2\pi/\lambda} \int_0^{2\pi} \left| \frac{\partial u_\theta}{\partial r} - \frac{u_\theta}{r} \right|_{r=R_1} R_1 \, d\theta \, d\zeta. \tag{12}$$

This becomes

$$G = G_0 \left| \frac{-2(1-\mu)}{\eta(1+\eta)} + \frac{(1+\eta)(1+\mu)}{4\eta} \frac{\partial v_0}{\partial x} \right|_{x=-1/2} \tag{13}$$

where $G_0 = 2\pi\rho\nu h R_1^3 \Omega_1 / d$, when the quantities given in (2)–(5) are introduced. Since G_0 carries the dimensions of G, G/G_0 is used hereafter as a dimensionless

torque (G_0 is in fact a constant multiple of the Couette torque). We have used the second order difference estimate of $\partial v_0/\partial x$ at $x = -\frac{1}{2}$ given by

$$\Delta x^{-1}(-1.5v_0(-\tfrac{1}{2}, t) + 2v_0(-\tfrac{1}{2} + \Delta x, t) - 0.5v_0(-\tfrac{1}{2} + 2\Delta x, t)).$$

Thus with $\mu = 0$, $\eta = 0.5$ we calculate

$$\frac{G}{G_0} = \left| -\frac{8}{3} + \frac{3}{4\Delta x}\left(2v_0\left(-\frac{1}{2} + \Delta x, t\right) - 0.5v_0\left(-\frac{1}{2} + 2\Delta x, t\right)\right)\right|. \quad (14)$$

Donnelly and Simon [9] developed an empirical torque relation (equation (22) of their paper) in which we replace Ω_1 with the Reynolds number $R = \Omega_1 R_1 d/\nu$ (using as appropriate to their data $\nu = 0.1226$ cm^2/sec, $\rho = 0.8404$ gm/cm^3, $h = 5.0$ cm) to obtain

$$G/G_0 = -2158\, R^{-2} + 1.452(0.1226\, R)^{0.364}. \quad (15)$$

Davey's analysis (1962) led to an equivalent of

$$G/G_0 = -5752\, R^{-2} + 3.908. \quad (16)$$

Figure 5 shows curves for (15) and (16) and data based on (14). A numerical version is contained in table I. The close agreement near $T/T_c = 1$ is to be expected. The

TABLE I

NONDIMENSIONAL TORQUE PER UNIT LENGTH (G/G_0) ON THE INNER CYLINDER FOR VARIOUS T/T_c AS GIVEN BY OUR CALCULATIONS AND THE RELATIONS GIVEN IN EQS. (14)–(16)

T/T_c	Present work	Davey	Donnelly and Simon
1.032	2.71	2.71	2.71
1.129	2.81	2.81	2.80
1.290	2.96	2.95	2.93
1.613	3.20	3.14	3.14
2.419	3.59	3.40	3.50
3.226	3.85	3.52	3.75
4.839	4.16	3.65	4.09

divergent trend observable as T/T_c increases may be due to the asymptotic nature of the analysis where Davey's curve is concerned. The discrepancy between our computed G/G_0 and the experimental values is probably within the bounds of

experimental error and due to a combination of experimental and numerical errors. As a test of overall numerical effectiveness, torque comparisons are unsatisfactory since they make use of only $\partial v_0/\partial x$ and that only at $x = -0.5$.

Recently, Snyder and Lambert [13] have reported measurements of the rate of strain at the inner cylinder. They analyzed these for harmonic (ζ-dependence) components and made comparisons with the same quantities computed from Davey's [4] tables. This rate of strain S is given by

$$S = \left[\left(\frac{\partial u_\theta}{\partial r} - \frac{u_\theta}{r}\right)^2 + \left(\frac{\partial u_z}{\partial r}\right)^2\right]^{1/2}\Bigg|_{r=R_1} \tag{17}$$

from which we derive

$$S/\Omega_1 = \frac{(1+\eta)(1+\mu)}{4(1-\eta)}\left\{\left[\frac{-8(1-\mu)}{(1+\eta)^2(1+\mu)} + \frac{\partial}{\partial x}\left(v_0 + \sum_{q=1}^{\infty} v_q \cos q\lambda\zeta\right)\right]^2 + \frac{(1+\mu)(1-\eta^2)}{2(\eta^2-\mu)\,T\lambda^2}\left[\sum_{q=1}^{\infty}\frac{1}{q}\frac{\partial^2 u_q}{\partial x^2}\sin q\lambda\zeta\right]^2\right\}^{1/2}\Bigg|_{x=-1/2} \tag{18}$$

for the dimensionless S/Ω_1. Using second-order differences for the derivatives, S/Ω_1 was approximated for ζ spaced uniformly from 0 to $2\pi/\lambda$ and to this data a truncated expansion $\sum_{q=0}^{Q} A_q \cos q\lambda\zeta$ was interpolated. The data given by Davey make the same procedure feasible using the equation

$$S/\Omega_1 = \frac{\eta}{1-\eta}\left\{\left[\frac{-2(1-\mu)}{\eta(1+\eta)} + A_e{}^2\frac{\partial}{\partial r}f_1(r) + A_e\frac{\partial v_1}{\partial r}\cos\lambda\zeta + A_e{}^2\frac{\partial v_2}{\partial r}\cos 2\lambda\zeta\right]^2 + \frac{1}{\lambda^2}\left[A_e\frac{\partial^2 u_1}{\partial r^2}\sin\lambda\zeta + \frac{1}{2}A_e{}^2\frac{\partial^2 u_2}{\partial r^2}\sin 2\lambda\zeta\right]^2\right\}^{1/2}\Bigg|_{r=R_1/d} + O(A_e{}^3). \quad \text{(Davey's notation).} \tag{19}$$

The quantity A_e is proportional to $(T - T_c)^{1/2}$ and so is small for T near T_c. We should emphasize that Davey's analysis is expected to be asymptotically valid only as $T \to T_c$ and takes into account only two harmonics while the present work includes up to six harmonics. The results are shown in Fig. 6 and table II.

Snyder and Lambert [13] describe the strengthening with increasing T of a jet of fluid moving radially outward between alternate vortex interfaces. This jet is characterized by increased radial velocity and narrowed axial channel as the speed of rotation of the inner cylinder is increased. Figure 7 shows radial velocity profiles of a single vortex at $x = 0$.

TABLE II

MEAN (A_0) AND HARMONICS (A_1 AND A_2) OF THE RATE OF STRAIN AT THE INNER CYLINDER FOR VARIOUS T/T_c AS GIVEN BY PRESENT CALCULATIONS AND TERMS THROUGH SECOND ORDER OF DAVEY'S EXPANSION

T/T_c	A_0		A_1		A_2	
	present	Davey	present	Davey	present	Davey
1.032	2.71	2.71	−.197	−.184	−.0219	−.0262
1.129	2.83	2.86	−.338	−.346	−.0686	−.0934
1.290	3.01	3.05	−.452	−.469	−.126	−.176
1.613	3.28	3.31	−.558	−.585	−.207	−.280
2.419	3.72	3.64	−.660	−.692	−.309	−.404
3.226	3.99	3.83	−.718	−.736	−.359	−.462
4.839	4.30	3.99	−.766	−.773	−.402	−.517

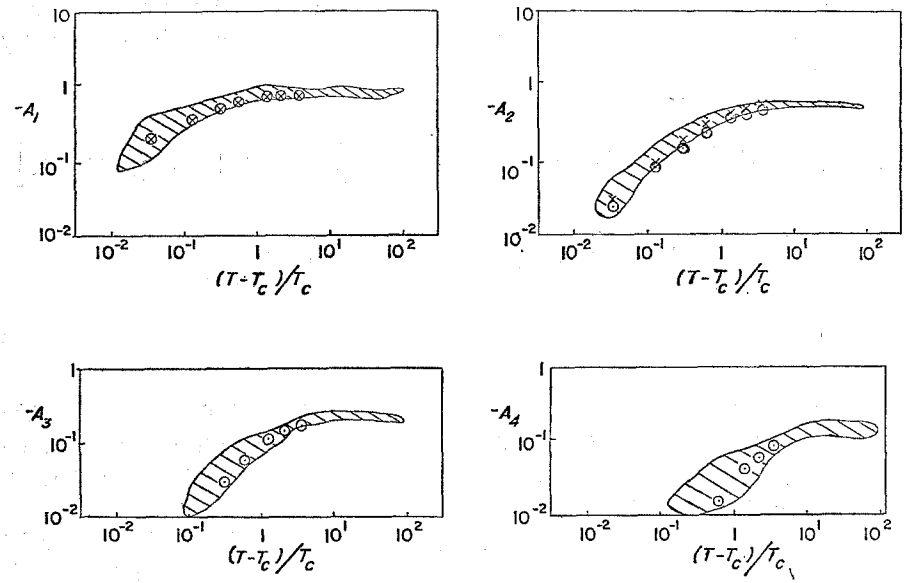

FIG. 6. Nondimensional harmonics A_1, A_2, A_3, A_4 of rate of strain at the inner cylinder versus $(T/T_c) - 1$; ⊙—present work; ×—Davey; shaded region—Snyder and Lambert experimental data.

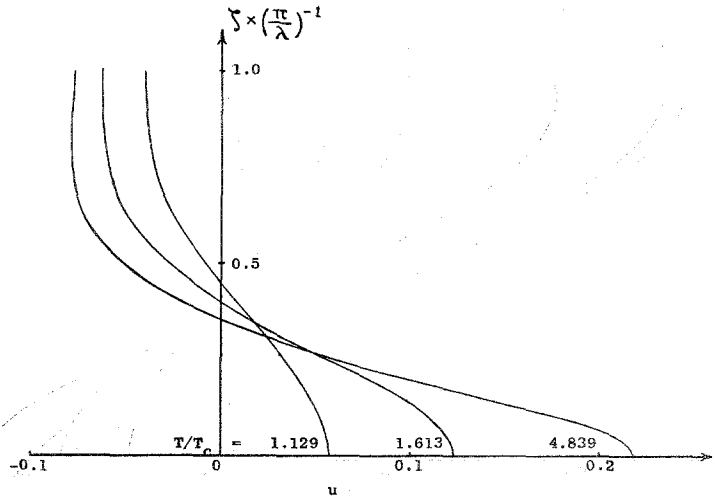

FIG. 7. Axial profile of total radial velocity midway between cylinders, showing growth of jet with T/T_c.

A parallel trend has been pointed out by Meyer [12]. This is the formation of shear layers in the circumferential flow, occurring at the same places as the jets. Clearly these are not independent developments, but Davey, DiPrima and Stuart [5] give an argument suggesting that this circumferential shear is the principal mechanism in the destabilization of Taylor vortices to a wavy vortex disturbance. Figure 8 shows the ratio of the angular fluid velocity at $x = 0$ (midcell) to that of the inner cylinder as a function of ζ for various T/T_c. Even though these calculations do not represent conditions approaching those at which the Taylor vortices become unstable, an interesting development is revealed. As T/T_c is increased, a velocity gradient develops, but not noticeably beyond $T/T_c = 1.613$ (see Fig. 8). However, in the $T/T_c = 3.226$ and 4.839 curves a growing reversal of curvature is discernable in the middle of the cells. This may be an early manifestation of the core of fluid moving with fixed angular velocity inside each vortex which Meyer found in his computation.

VI. REMARKS

A few comments about the numerical method are in order here. Advantage has been taken of a somewhat special situation. The fluid flow studied was known to be periodic in the ζ-direction and the flow was expected to be composed principally of low order harmonics for T near T_c. The latter expectation is crucial. It means

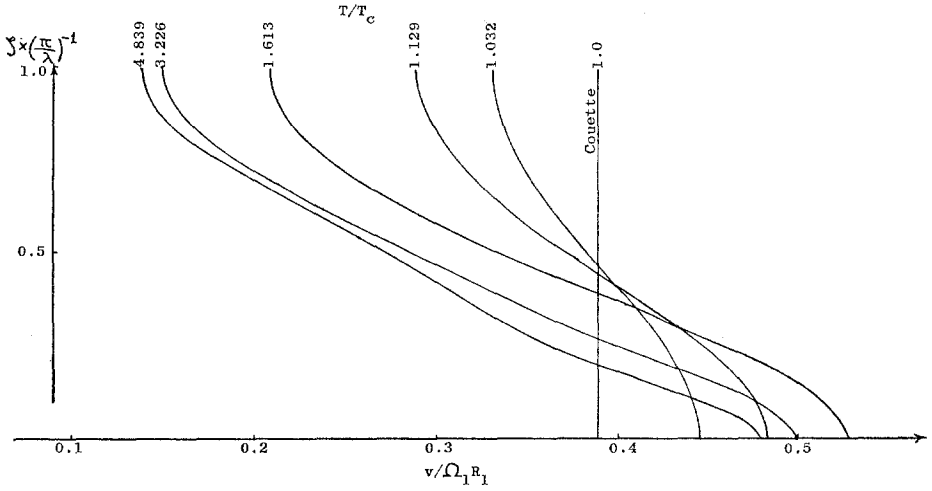

FIG. 8. Ratio of circumferential velocity to velocity $\Omega_1 R_1$ of inner cylinder midway between cylinders.

that the number Q of harmonics used in the numerical study for a given accuracy will be smaller than the number of axial mesh levels required in a pure differencing for comparable accuracy. Without such an expection the use of a truncated Fourier series has no advantage over a direct differencing of the dependent variables in all spatial directions.

Conceivably, expansions in functions other than the trigonometric might be profitably used when they can be seen to have a natural association with the problem under study. These functions might occur as eigenfunctions of a related boundary value problem, for instance.

ACKNOWLEDGMENTS

The authors wish to express their gratitude to Professors R. C. DiPrima and L. A. Segel for their valuable counsel and to acknowledge the generous availability of the Rensselaer Polytechnic Institute computer facilities (IBM 360/50). In addition, the Army Research Office (Durham) and the Office of Naval Research are thanked for their support.

APPENDIX

Nonlinear Terms.

The nonlinear terms appearing in equations (7) and (8) are given by

$$\begin{aligned}
U_q = -\frac{1}{\alpha}\Big\{ & -q^2\lambda^2\frac{\alpha T\xi}{\delta}v_0v_q \\
& + \frac{1}{2}\sum_{j=1}^{q-1}\Big[-\frac{q}{q-j}DD^*(u_jD^*u_{q-j}) + \frac{q^2}{j(q-j)}D((D^*u_j)(D^*u_{q-j})) \\
& + q^2\lambda^2D^*(u_ju_{q-j}) - q^2\lambda^2\frac{\alpha T\xi}{2\delta}(v_jv_{q-j}) - \frac{q}{q-j}q^2\lambda^2u_jD^*u_{q-j}\Big] \\
& + \frac{1}{2}\sum_{j=q+1}^{\infty}\Big[\frac{q}{j-q}DD^*(u_jD^*u_{j-q}) - \frac{q^2}{j(j-q)}D((D^*u_j)(D^*u_{j-q})) \\
& + q^2\lambda^2D^*(u_ju_{j-q}) - q^2\lambda^2\frac{\alpha T\xi}{2\delta}(v_jv_{j-q}) + \frac{q}{j-q}q^2\lambda^2u_jD^*u_{j-q}\Big] \\
& + \frac{1}{2}\sum_{j=1}^{\infty}\Big[-\frac{q}{j+q}DD^*(u_jD^*u_{j+q}) - \frac{q^2}{j(j+q)}D((D^*u_j)(D^*u_{j+q})) \\
& + q^2\lambda^2D^*(u_ju_{j+q}) - q^2\lambda^2\frac{\alpha T\xi}{2\delta}(v_jv_{j+q}) - \frac{q}{j+q}q^2\lambda^2u_jD^*u_{j+q}\Big]\Big\}
\end{aligned}$$

and

$$\begin{aligned}
V_q = \frac{1}{\alpha}\Big\{ & (D^*+\xi)(v_0u_q) - v_0D^*u_q \\
& + \frac{1}{2}\sum_{j=1}^{q-1}\Big[(D^*+\xi)(u_jv_{q-j}) - \frac{q}{j}(D^*u_j)\,v_{q-j}\Big] \\
& + \frac{1}{2}\sum_{j=q+1}^{\infty}\Big[(D^*+\xi)(u_jv_{j-q}) - \frac{q}{j}(D^*u_j)\,v_{j-q}\Big] \\
& + \frac{1}{2}\sum_{j=1}^{\infty}\Big[(D^*+\xi)(u_jv_{j+q}) + \frac{q}{j}(D^*u_j)\,v_{j+q}\Big]\Big\}.
\end{aligned}$$

Finite Differences.

The operators P and M contain differentiations only in the combinations DD^* and $(DD^*)^2$. Using $D^k\xi = (-1)^k\,k!\,\xi^{k+1}$, we note

$$(DD^*)f = D^2f + \xi Df - \xi^2f$$

and

$$(DD^*)^2f = D^4f + 2\xi D^3f - 3\xi^2D^2f + 3\xi^3Df - 3\xi^4f.$$

The difference operators $\hat{P}$ and $\hat{M}$ are constructed by replacing the differentiation operators D, D^2, D^3, D^4 by the difference operators defined by

$$Df(-\tfrac{1}{2} + j\Delta x) \sim (-f_{j-1} + f_{j+1})/2\Delta x,$$
$$D^2f(-\tfrac{1}{2} + j\Delta x) \sim (f_{j-1} - 2f_j + f_{j+1})/\Delta x^2,$$
$$D^3f(-\tfrac{1}{2} + j\Delta x) \sim (-f_{j-2} + 2f_{j-1} - 2f_{j+1} + f_{j+2})/2\Delta x^3,$$
$$D^4f(-\tfrac{1}{2} + j\Delta x) \sim (f_{j-2} - 4f_{j-1} + 6f_j - 4f_{j+1} + f_{j+2})/\Delta x^4.$$

The treatment of D and D^* in the nonlinear terms is the same. However, differentiation of products of the dependent variables occur there. We have elected to expand the differentiations according to the product rule until D, D^2, D^3 apply only to single dependent variables. For instance,

$$DD^*(f(D^*g)) = (D^2f)(Dg) + 2(Df)(D^2g) + fD^3g + \xi[(D^2f)g + 3(Df)(Dg) + 2fD^2g] - \xi^2[(Df)g + 2fDg]$$

occurs in U_q with $f = u_j$, $g = u_{q-j}$. The simple difference formulas given above are substituted.

References

1. G. Capriz, G. Ghelardoni, and G. Lombardi, *Phys. Fluids* **9**, 1934 (1966).
2. S. Chandrasekhar, "Hydrodynamic and Hydromagnetic Stability." Oxford University Press (1960).
3. D. Coles, *J. Fluid Mech.* **21**, 385 (1965).
4. A. Davey, *J. Fluid Mech.* **14**, 336 (1962).
5. A. Davey, R. C. DiPrima, and J. T. Stuart, *J. Fluid Mech.* **31**, 17 (1968).
6. R. C. DiPrima, *J. Appl. Mech.* **30**, 486 (1963).
7. R. C. DiPrima, *in* "Nonlinear Partial Differential Equations" (W. F. Ames, Ed.). Academic Press (1967).
8. R. C. DiPrima and E. H. Rogers, *Phys. Fluids* (to appear).
9. R. J. Donnelly and N. Simon, *J. Fluid Mech.* **7**, 401 (1960).
10. H. Görtler and W. Velte, *Phys. Fluids Suppl.* **S3** (1967).
11. A. L. Krilov and E. K. Proizvolova, *Proc. Computing Centre Moscow Univ.* **2**, 174 (1963).
12. K. Meyer, Los Alamos Report LA-3497 (1966); *Phys. Fluids* **10**, 1874 (1967).
13. H. A. Snyder and R. B. Lambert, *J. Fluid Mech.* **26**, 545 (1966).